Accurate *ab initio* density fitting for multiconfigurational self-consistent field methods

Francesco Aquilante,[1,a)] Thomas Bondo Pedersen,[1,b)] Roland Lindh,[1] Björn Olof Roos,[1] Alfredo Sánchez de Merás,[2] and Henrik Koch[3]

[1]*Department of Theoretical Chemistry, Chemical Center, University of Lund, P.O. Box 124, S-221 00 Lund, Sweden*
[2]*Institute of Molecular Science, Department of Physical Chemistry, University of Valencia, E-46100 Burjassot, Valencia, Spain*
[3]*Department of Chemistry, Norwegian University of Science and Technology, N-7491 Trondheim, Norway*

Using Cholesky decomposition and density fitting to approximate the electron repulsion integrals, an implementation of the complete active space self-consistent field (CASSCF) method suitable for large-scale applications is presented. Sample calculations on benzene, diaquo-tetra-μ-acetato-dicopper(II), and diuraniumendofullerene demonstrate that the Cholesky and density fitting approximations allow larger basis sets and larger systems to be treated at the CASSCF level of theory with controllable accuracy. While strict error control is an inherent property of the Cholesky approximation, errors arising from the density fitting approach are managed by using a recently proposed class of auxiliary basis sets constructed from Cholesky decomposition of the atomic electron repulsion integrals. © *2008 American Institute of Physics.*
[DOI: 10.1063/1.2953696]

I. INTRODUCTION

The success of correlated wave function theories is inextricably linked to the quality of the underlying mean-field description of the electronic structure. While the Hartree–Fock (HF) wave function often is a good starting point for correlated treatments of molecular electronic structure, understanding the true nature of the chemical bond requires a more general mathematical formulation at the mean-field level. The insufficient account of static electron correlation is the reason behind the failure of the HF reference wave function in many situations. Systems such as molecules with unfilled valencies in their electronic ground state (e.g., radicals and diradicals) or molecules containing atoms with low-lying excited states possess a number of near degenerate electronic configurations and therefore exhibit strong static correlation effects. More generally, at the dissociation limit for chemical bonds, along reactions paths in chemical and photochemical reactions, and often for excited electronic states, a qualitatively correct description of the wave function is possible only if the most significant electronic configurations are included.

The natural way to extend the HF model to account for static correlation effects is therefore to construct the mean-field electronic wave function from multiple Slater determinants. This approach results in a multiconfigurational self-consistent field (MCSCF) wave function. The increased complexity of the MCSCF wave function is accompanied by a sizable increase in computational cost compared to the HF wave function. The computational cost can be kept at a reasonable level by selecting a small number of electrons and orbitals, the so-called active space, and include in the MCSCF wave function all possible electronic configurations obtained by distributing these active electrons into the active orbitals. This leads to the complete active space self-consistent field (CASSCF) wave function.[1] Given a physically correct active space, the CASSCF wave function offers maximum flexibility for a qualitative description of the electronic structure of even the most exotic types of chemical bonds.[2] The dynamical correlation required for a quantitative description can be recovered by a subsequent second-order perturbative correction (CASPT2).[3] The success of this approach has been documented by a number of studies on electronic ground (see, e.g., Refs. 4 and 5) and excited states (see, e.g., Refs. 6–10). In addition, the CASSCF wave function has been instrumental for understanding photochemical processes.[11,12]

The sheer number of electronic configurations is the major obstacle to the application of the CASSCF method to large molecules. In many cases, however, relatively small active spaces can be devised independently of the size of the molecule. In such cases, the bottleneck of CASSCF calculations is the evaluation and storage of electron repulsion integrals (ERIs) in atomic orbital (AO) basis and their transformation to molecular orbital (MO) basis. In fact, as for other correlated wave-function-based methods, rather large one-electron basis sets must be used to obtain converged results for the total CASSCF/CASPT2 correlation energy. It is therefore of utmost importance to develop techniques that can reduce the computational cost of calculating and transforming the ERIs.

a)Present address: Department of Physical Chemistry, Sciences II, University of Geneva, Quai E. Ansermet 30, 1211 Geneva 4, Switzerland. Electronic mail: francesco.aquilante@teokem.lu.se.
b)Present address: Atomistix A/S, c/o Niels Bohr Institute, Rockefeller Complex, Juliane Maries Vej 30, DK-2100 Copenhagen, Denmark.

As the ERI matrix is symmetric positive semidefinite, Cholesky decomposition (CD) can be used to reduce storage as well as computational demands.[13,14] When the resulting Cholesky vectors are employed directly in the evaluation of Fock matrices and ERIs in the MO basis, the computational cost of *ab initio* and density functional theory (DFT) methods drops considerably.[14–16] Nearly abandoned for almost three decades,[17–19] the CD approach has now been integrated in modern quantum chemistry softwares and proven to be an excellent approximation for fast and accurate correlated calculations.[14,15,20–30] In this work, we demonstrate that the CD approach can be used also in conjunction with the CASSCF method.

The density fitting (DF) or resolution of the identity[31–33] (RI) approximation is a much more widespread technique for handling ERIs in computational quantum chemistry. For example, DF has been used to speed up DFT and second-order Møller–Plesset (MP2) energy[34–40] and property[41–44] calculations. Unlike the CD approach, however, DF requires an auxiliary basis set for expanding AO product densities. The auxiliary basis sets are normally designed to be used with a particular method and AO basis set in such a way that specific energy contributions are accurately represented.[35,41,45,46] However, as pointed out by Ten-no and Iwata,[47,48] such procedure is hardly meaningful for the CASSCF method, as it would probably require different auxiliary basis sets to accurately approximate the MO-transformed ERIs needed in CASSCF as well as the Coulomb and exchange contributions from the inactive and active Fock matrices. Moreover, the dependence of the computed energy on the choice of the active space makes it very difficult to set up a consistent optimization procedure of the type required for externally defined auxiliary basis sets.

Recently, three of the present authors have proposed the atomic CD (aCD) approach for generating hierarchies of auxiliary basis sets that are not biased towards a particular quantum chemical method.[49] These aCD auxiliary basis sets were shown to give accurate ground state energies with HF, MP2, and hybrid as well as nonhybrid DFT methods.[49] In the present work, we investigate their accuracy and efficiency in conjunction with the CASSCF wave function.

Section II presents an implementation of the CASSCF equations based on CD or DF ERI approximations. Sample CASSCF calculations demonstrating the accuracy and performance of the new implementation are given in Sec. III, and our conclusions are given in Sec. IV.

II. THEORY

A. CD and DF representations of the ERIs

The ERIs in AO basis can be written as

$$(\mu\nu|\lambda\sigma) \simeq \sum_{J=1}^{M} L_{\mu\nu}^{J} L_{\lambda\sigma}^{J}, \tag{1}$$

where Greek indices represent the AOs χ_μ. The vectors $\mathbf{L}^J$ are calculated either by a CD of the ERI matrix or by a DF procedure.

In the CD case, the vectors are calculated recursively according to[13,14]

$$L_{\mu\nu}^{J} = (\widetilde{h_J|h_J})^{-1/2} \left[(\mu\nu|h_J) - \sum_{K=1}^{J-1} L_{\mu\nu}^{K} L_{J}^{K} \right], \tag{2}$$

$$(\widetilde{h_J|h_J}) = (h_J|h_J) - \sum_{K=1}^{J-1} (L_J^K)^2, \tag{3}$$

for $J = 1, 2, \ldots, M$. Each of the functions in the Cholesky basis $\{h_J\}$ is a specific AO product function $\chi_\lambda\chi_\sigma$ selected in each step J of the CD procedure by the criterion $(h_J\widetilde{|}h_J) = \max_{\lambda\sigma}(\lambda\sigma\widetilde{|}\lambda\sigma)$. The recursive procedure is completed once the largest updated diagonal ERI matrix element is smaller than the decomposition threshold $\delta \geq 0$, i.e., $(h_J\widetilde{|}h_J) \leq \delta$. Hence, M is the number of Cholesky vectors needed to represent all ERIs with an accuracy of at least δ. See Refs. 13 and 14 for more details of the CD procedure.

The DF vectors can be calculated according to

$$L_{\mu\nu}^{J} = \sum_{K} (\mu\nu|h_K) B_{KJ}, \tag{4}$$

where the matrix $\mathbf{B}$ is the inverse Cholesky factor of the matrix

$$G_{JK} = (h_J|h_K). \tag{5}$$

That is,

$$\mathbf{G}^{-1} = \mathbf{B}\mathbf{B}^{T}, \tag{6}$$

where the superscript T denotes matrix transposition. In contrast to the CD procedure, the DF approach requires the definition of an auxiliary basis set $\{h_J\}$. Traditional auxiliary basis sets consist of atom-centered (contracted) Gaussian functions whose exponents (and contraction coefficients) are optimized for each AO basis set and quantum chemical method, see, e.g., Refs. 35, 46, 50, and 51. Ten-no and Iwata[47,48] proposed a different approach for generating auxiliary basis sets. In this approach, the atomic ERI matrix is diagonalized and all eigenvectors corresponding to eigenvalues above a given threshold are used as auxiliary basis functions. Recently, three of the authors[49] proposed a similar procedure for generating auxiliary basis sets. Instead of diagonalization, the atomic ERI matrix is Cholesky decomposed and the resulting Cholesky basis defines the auxiliary basis set. Performing a range of aCDs with decreasing decomposition threshold δ leads to hierarchies of increasingly accurate auxiliary basis sets. The aCD procedure for generating auxiliary basis sets is performed on the fly for each unique atom/AO basis set pair. Since the Cholesky (auxiliary) basis set $\{h_J\}$ in both CD and aCD is not obtained through any data fitting but instead systematically derived from the AO basis set, it seems appropriate to refer to this type of approaches in a unified language as "*ab initio* density fitting." We here use two different types of aCD auxiliary basis sets. The aCD-n* auxiliary basis set is generated by aCD with decomposition threshold $\delta = 10^{-n}$. The aCD-n auxiliary basis set is obtained from the aCD-n* set by removing

the highest angular momentum functions. More details can be found in Ref. 49.

For both CD and aCD, the number of vectors, M, is comparable to the number of AOs, N. Depending primarily on the decomposition threshold and much less on the type of the AO basis set, typical values of the ratio M/N range from 3 to 8.

B. The CASSCF method using CD and DF

We base our discussion on the formulation of the CASSCF method as described in detail in Ref. 52. The standard notation for MO indices is used: $i,j,k,l,\dots$ refer to inactive, $t,u,v,w,\dots$ to active, $a,b,c,d,\dots$ to secondary, and m,n,p,q,r,s to general MO indices.

Defining the MCSCF Fock operator with matrix elements

$$F_{mn} = \sum_q D_{mq}h_{nq} + \sum_{qrs} P_{mqrs}(nq|rs),\qquad(7)$$

the Brillouin–Levy–Berthier conditions can be written as

$$F_{ia} = 0,$$
$$F_{ta} = 0,\qquad(8)$$
$$F_{it} - F_{ti} = 0,$$

where **D** and **P** are the one- and two-electron density matrices, and **h** is the one-electron Hamiltonian. These equations represent the set of necessary and sufficient conditions for optimal orbitals in the CASSCF wave function. The expression of the non-Hermitian generalized Fock matrix in Eq. (7) is completely general and is valid for any kind of wave function. In the CASSCF case, however, it is possible to rewrite this Fock matrix in such a way that only density matrix elements with all indices active are referenced. In fact, when the first index refers to an inactive orbital, we can write

$$F_{in} = 2({}^I F_{ni} + {}^A F_{ni})\qquad(9)$$

once we define the following (Hermitian) inactive and active Fock matrices:

$${}^I F_{mn} = h_{mn} + \sum_k [2(mn|kk) - (mk|kn)],\qquad(10)$$

$${}^A F_{mn} = \sum_{vw} D_{vw}\left[(mn|vw) - \frac{1}{2}(mw|vn)\right].\qquad(11)$$

If the first index belongs instead to an active orbital, we obtain

$$F_{vn} = \sum_w D_{vw}\,{}^I F_{nw} + Q_{vn},\qquad(12)$$

where we have introduced the matrix **Q** given by

$$Q_{vm} = \sum_{wxy} P_{vwxy}(mw|xy),\qquad(13)$$

Finally, we can easily prove that the Fock matrix elements vanish whenever the first index belongs to the secondary space.

In the conventional CASSCF approach, the inactive and the active Fock matrices are computed in the AO basis while the **Q** matrix is directly computed from the list of MO-transformed integrals. For relatively small configuration expansions and large atomic basis sets, the integral transformation is the bottleneck of the CASSCF calculations, scaling as AN^4, where A is the number of active orbitals.

Using the ERI expression of Eq. (1), it is possible to compute the inactive and active Fock matrices, Eqs. (10) and (11), in the AO basis in the same way as in CD-based HF,[14,16]

$$F_{\lambda\sigma} = \sum_J L_{\lambda\sigma}^J \sum_{\mu\nu} D_{\mu\nu} L_{\mu\nu}^J - \frac{1}{2}\sum_{kJ} L_{k\lambda}^J L_{k\sigma}^J,\qquad(14)$$

where k runs over either the inactive (${}^I F$) or the active (${}^A F$) orbital indices, and **D** is the corresponding one-electron density matrix in the AO basis. The formal scaling (leading term) of the evaluation of both these matrices is $(I+A)N^2M$, where I is the number of inactive orbitals. The quartic scaling is due to the evaluation of the exchange terms which require also a MO half-transformation of the vectors, $L_{\lambda\sigma}^J \rightarrow L_{k\lambda}^J$. By using the recently developed "local exchange" (LK) screening[16] in conjunction with localized Cholesky MOs,[53] the actual scaling of this step is reduced to quadratic even in compact molecules.[16]

The construction of the **Q** matrix is done without explicit construction of the MO-transformed ERIs. The **Q** matrix can be computed more efficiently using the following half-transformed expression:

$$Q_{v\alpha} = \sum_{wJ} L_{\alpha w}^J \sum_{xy} P_{vwxy} L_{xy}^J = \sum_{wJ} L_{\alpha w}^J Z_{vw}^J,\qquad(15)$$

where the leading term scales as A^2NM.

Integrals of the type $(tw|xy)$ are needed for the solution of the CAS-CI secular equations and they can be easily generated from the fully transformed (in the active space) vectors. The cost of the integral generation scales as A^4M.

The bottleneck in the construction of the CASSCF Fock matrix and $(tw|xy)$ integrals is moved from the MO integral transformation to the evaluation of the inactive exchange Fock matrix. Thus, all the well known advantages of using the DF and CD approximations in the HF method[16,51,54] are present also in CASSCF and, hence, large-scale applications of the latter become possible.

As shown in the Appendix, another strategy for implementing DF and CD approximations in CASSCF would be to construct the inactive and active Fock matrices directly as MO half-transformed quantities. Solely based on an operation count viewpoint, such algorithm would be advantageous compared to the one previously described. On the other hand, the LK screening reduces drastically the number of contributions effectively computed. In terms of overall speed of the calculation, it is therefore necessary to complement the second algorithm with an equally efficient screening technique. In this respect, the evident analogy between the two algorithms seems to indicate that a slightly modified version of the LK screening would meet such requirements. We intend to return to this subject in future publications,

TABLE I. Benzene molecule. Deviations with respect to conventional calculations of the state-averaged π-CASSCF total energies. Ground and two lowest-lying excited singlet electronic states of A_{1g} symmetry. Total numbers of AO basis functions: 114 (cc-pVDZ), 264 (cc-pVTZ), and 510 (cc-pVQZ).

	ΔE/meV								
	$1\ ^1A_{1g}$			$2\ ^1A_{1g}$			$3\ ^1A_{1g}$		
Vectors	cc-pVDZ	cc-pVTZ	cc-pVQZ	cc-pVDZ	cc-pVTZ	cc-pVQZ	cc-pVDZ	cc-pVTZ	cc-pVQZ
CD-3	193.94	−111.16	13.82	206.13	−98.36	16.32	199.09	97.96	15.45
CD-4	4.40	13.56	−10.53	4.52	13.94	−10.23	4.28	13.35	10.52
CD-5	0.73	1.32	0.08	0.86	1.31	0.13	0.87	1.25	0.05
aCD-3*	0.70	5.52	8.46	0.55	5.95	8.66	0.30	5.56	8.54
aCD-4*	0.59	0.13	8.29	0.46	0.13	8.49	0.14	0.09	8.36
aCD-5*	1.78	0.14	8.21	2.13	0.14	8.41	2.00	0.10	8.28
aCD-3	1.68	−34.94	−586.60	0.87	−47.31	−664.14	−0.53	−50.63	−673.90
aCD-4	6.42	−67.19	82.59	4.24	−82.40	72.29	3.11	−82.91	55.19
aCD-5	7.73	−58.25	48.99	7.15	−71.12	31.24	6.60	−70.70	16.22

whereas here we have only implemented the formulas of the present section in order to make use of existing codes for the self-consistent wave function optimization.

III. SAMPLE CALCULATIONS

In this section we present sample CASSCF calculations for three molecules. The benzene molecule, which is a standard system for benchmarking the ability of CASSCF to describe both ground and excited states,[55–57] is used to assess the accuracy of the CD and DF-based CASSCF. The superior performance of the new implementation is verified by comparing conventional and CD and DF timings for calculating the magnetic coupling constant of an antiferromagnetic Cu(II) complex, diaquo-tetra-μ-acetato-dicopper(II). Finally, calculations of diuraniumendofullerene demonstrate the large-scale applicability of the CD and DF-based CASSCF. All calculations are performed on a single AMD Opteron 2.4 GHz processor with a development version of the MOLCAS quantum chemistry software.[58,59]

A. Benzene

The calculations on the benzene molecule use Dunning's correlation consistent basis sets[60] and are performed within the D_{2h} point group symmetry, which is the largest Abelian subgroup of the full D_{6h} point group of benzene. The states are labeled according to the irreducible representations of the latter. Using six electrons and the six π and π^* orbitals as active space, a typical choice for small unsaturated hydrocarbons, we optimize the state-averaged π-CASSCF wave functions of the three lowest-lying A_{1g} singlet electronic states of benzene. The ground state, $1\ ^1A_{1g}$, is dominated (87%) by the HF electronic configuration. The first excited state, $2\ ^1A_{1g}$, is described by a mixture of two single-excited configurations $(31\% + 14\%)$ and by the HF electronic configuration (20%). Its energy is predicted to be 7.82 eV above the ground state with the cc-pVQZ basis set and 7.89 or 7.84 eV with cc-pVDZ or cc-pVTZ, respectively. The second excited state, $3\ ^1A_{1g}$, is dominated by two double-excited configurations $(21\% + 21\%)$ with a significant contribution from the HF electronic configuration (24%). The computed energy of this

second excited state is 11.27 eV above the ground state with the cc-pVQZ basis set and 11.39 or 11.30 eV with cc-pVDZ or cc-pVTZ, respectively. It may be argued that these two excited states are not the most relevant from a spectroscopic point of view. Indeed, with this example we aimed at testing the accuracy of our method in rather extreme situations, thus for CASSCF states of high energy and multiconfigurational character.

Tables I and II report the errors of various CD and DF approximations with respect to conventional results for total energies and excitation energies, respectively. Representing the ERIs by a CD of threshold $\delta = 10^{-n}$ is denoted CD-n in these tables. Evidently, CD and DF-based CASSCF produces accurate results, especially for excitation energies (i.e., energy differences) which benefit from error cancellation. Preliminary calculations on triplet states as well as other singlet states of benzene have shown similar accuracies. In particular, for the aCD-n* sets, we observe an error in the computed excitation energies of at most 0.44 meV and note that the error nearly vanishes with the largest (cc-pVQZ) basis set. This range of errors is well below the inherent error due to truncation of the one-electron basis set. For instance, the largest difference in the excitation energies computed with cc-pVDZ and cc-pVQZ in the present example is about 120 meV, three orders of magnitude larger than the maximum error introduced by the most accurate CD and DF approximations $(\delta = 10^{-5})$.

From Table I we notice a major difference between the CD and aCD approximations. The CD shows invariably better accuracy in the total computed energy when using tighter thresholds. The same is not always true for the aCD* basis sets and seems to be not at all a property of the reduced aCD basis sets. This can be explained by the fact that in the aCD approximations, the inaccuracy of the two-electron integrals is no longer bounded by the decomposition threshold and therefore the resulting errors in the energy can have a somewhat accentuated statistical behavior. In Fig. 1, we report the maximum and root mean square (rms) error in the value of the diagonal elements of the ERI matrix of benzene (C_1 point group symmetry) employing aCD* auxiliary functions for the cc-pVTZ valence basis set. The general trend (accuracy

TABLE II. Benzene molecule. Deviations with respect to conventional calculations of the state-averaged π-CASSCF excitation energies of A_{1g} symmetry. Total numbers of AO basis functions: 114 (cc-pVDZ), 264 (cc-pVTZ), and 510 (cc-pVQZ).

	$\Delta(E-E_0)$/meV					
	$1\,^1A_{1g}\rightarrow 2\,^1A_{1g}$			$1\,^1A_{1g}\rightarrow 3\,^1A_{3g}$		
Vectors	cc-pVDZ	cc-pVTZ	cc-pVQZ	cc-pVDZ	cc-pVTZ	cc-pVQZ
CD-3	12.18	12.80	2.50	5.14	13.20	1.63
CD-4	0.12	0.38	0.29	−0.12	−0.21	0.00
CD-5	0.12	−0.01	0.05	0.13	−0.06	0.02
aCD-3*	−0.15	0.42	0.19	−0.40	0.03	0.08
aCD-4*	−0.13	0.00	0.19	−0.44	−0.04	0.07
aCD-5*	0.35	0.00	0.19	0.21	−0.03	0.07
aCD-3	−0.80	−12.37	−77.53	−2.21	−15.69	−87.29
aCD-4	−2.17	−15.20	−10.30	−3.31	−15.71	−27.40
aCD-5	−0.58	−12.86	−17.35	−1.13	−12.45	−32.77

versus decomposition threshold) in the representation of the ERIs is respected. The histograms of Fig. 1 should be analyzed together with the diagram of Fig. 2 where the number of auxiliary functions (M) employed in the various DF representations is plotted as a function of decomposition threshold. The aCD* sets contain more functions than the corresponding CD and therefore it is not surprising that aCD-3* in
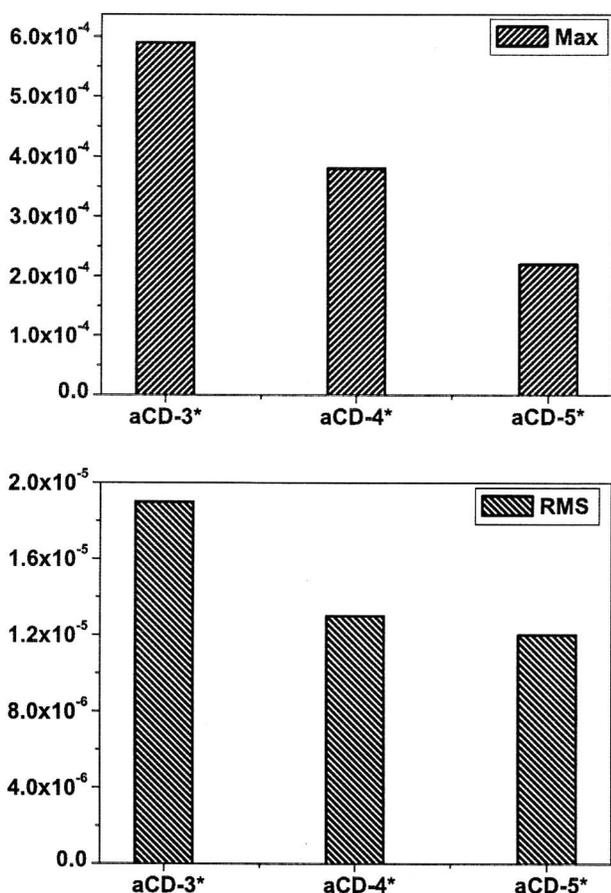

FIG. 1. Benzene molecule. Maximum and rms errors in the representation of the diagonal AO two-electron integrals employing various aCD approximations for the cc-pVTZ basis set. Notation described in the text.

Fig. 1 gives an accuracy in the integral representation on the order of 10^{-4}, even better than expected for the CD-3 representation. We also note that the corresponding error for the aCD-3 auxiliary basis set is on the order of 10^{-2}, indicating that some of the integrals are poorly approximated once the highest angular components are removed from the atomic auxiliary basis sets. Regarding these reduced aCD basis sets, two important things can be deduced from Fig. 2. First, they contain much less functions than the corresponding aCD* basis sets and, second, the number of such functions is nearly independent of the chosen decomposition threshold. We also point out that occasionally, as in the case reported in Fig. 2, the number of auxiliary functions in the aCD sets does not necessarily increase when larger valence basis sets are employed. These observations guide us to a better understanding of Table I. Except for the tighter thresholds, each aCD* set gives an improved approximation over the corresponding CD. This is surprisingly true also for the aCD sets, although the errors become relatively larger for the cc-pVQZ calculations. Most importantly, these errors seem to be very consistent between the various electronic states, an observation
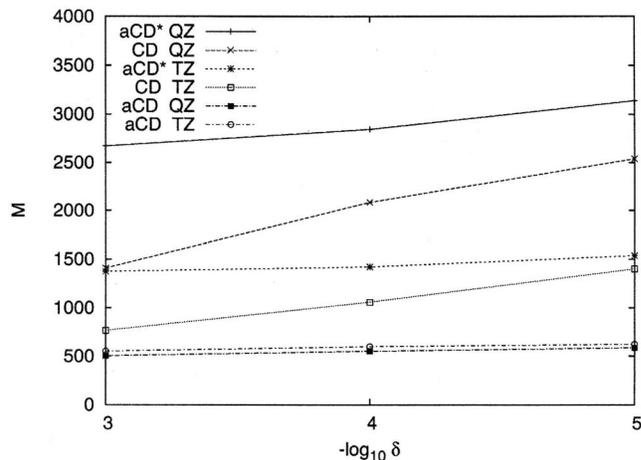

FIG. 2. Benzene molecule. Number of CD and aCD auxiliary basis functions needed at a given decomposition threshold for cc-pVXZ basis sets (X=T,Q).

confirmed by the results of Table II. Here, the benefits of error cancellations are clear since at all levels of DF approximation, we observe a much higher accuracy in the computed excitation energies than for the corresponding total energies. It should be mentioned that the accuracy of the results of Tables I and II is also affected by the fact that CASSCF is an iterative energy minimization procedure and not just a single energy calculation (not forgetting that there is also a preliminary SCF wave function optimization involved). If all the CASSCF energy calculations had been performed with the same set of starting orbitals (say, optimized conventional CASSCF orbitals), the overall accuracy would have been improved further. For real-life applications, however, the results reported here are certainly of greater interest.

We conclude from the results of Table II that all DF approximations introduced in the present work are reliable for predicting the excitation energies at the CASSCF level of theory. While the CD approximation is the most robust among them, the use of the aCD auxiliary basis sets would result in the computationally most efficient choice due to the minimal number of auxiliary functions required. The aCD* sets are very accurate even at loose thresholds and although they constitute a larger auxiliary basis set than their CD counterparts, the possibility to avoid the somewhat expensive decomposition of the molecular ERI matrix can often be an advantage, as discussed below.

A more thorough study on the accuracy of the CD approximation in spectroscopy was recently performed on the low-lying excited states of the complex Co(III) (di-iminato)(NPh). We refer to Ref. 29 for details of the calculations and the results. Here, we just want to mention that with an ANO-RCC-VTZP basis set (869 functions), on the type of hardware specified above, the time needed to generate the CD vectors (CD-4) was 217 min and the iteration time for the CASSCF calculations (ten active orbitals with ten electrons) was 4 min per iteration. The errors in computed excitation energies for 24 electronic states was never larger than 0.01 eV.

B. Diaquo-tetra-μ-acetato-dicopper(II)

We demonstrate the computational advantages in using CD and DF-based CASSCF over conventional implementations by calculating the magnetic coupling constant (J) as the energy difference between the lowest-lying singlet (E_S) and triplet (E_T) electronic states of one of the first synthetic molecular magnetic material, diaquo-tetra-μ-acetato-dicopper(II) (see Ref. 61 and references therein). This complex exhibits an antiferromagnetic behavior with an experimentally well characterized magnetic coupling constant of $J=-37$ meV. A minimal active space of two electrons and two orbitals can qualitatively describe the physics of the problem, especially if a sufficiently large AO basis set is employed. We here use the 6-3111+G(f) basis set on Cu and the 6-31G* basis set on the remaining atoms. The conventional calculation yields $E_S=-4338.692\ 123\ 02$ a.u., $E_T=-4338.692\ 035\ 57$ a.u., and $J=-2.379$ meV. Although outside the scope of the present

TABLE III. $\{C_{14}(H_2O)\}_2(\mu\text{-AcO})_4$, C_1 point group symmetry. Absolute errors with respect to conventional single-state CASSCF(2,2) energies of the lowest singlet (E_S) and triplet (E_T) states and magnetic coupling constant ($J=E_S\text{-}E_T$). A total of 394 AO basis functions was employed.

Vectors	Wall time (h) (disk/Gb)	Absolute deviation (meV)		
		E_S	E_T	J
Conventional	9.8 (19)	…	…	…
CD-8	2.1(1.4)	0.0095	0.0097	0.000
CD-6	1.2(1.1)	0.574	0.571	0.003
CD-4	0.5(0.8)	73.392	73.395	0.003
aCD 4*	0.9(1.1)	47.749	47.736	0.013
aCD-4	0.4(0.6)	106.49	106.49	0.000

work, we note that it is necessary to include dynamical correlation effects in order to reproduce the experimental magnetic coupling constant.

Due to the relatively small energy difference, it is crucial that the inaccuracy introduced by CD or DF is minimal. This is clearly the case, as can be seen from Table III. The error in the computed J is in all cases below 0.02 meV and effectively zero for most of them. This is mainly due to error cancellation, as the total energy deviations are one to two orders of magnitude larger depending on the chosen threshold for CD or aCD. Table III also reports the wall time and disk space required to perform the two single-state CASSCF calculations. (Timings include the integral/vector generation but not the preliminary SCF calculation. All 12 CASSCF calculations converge in nine iterations.) The largest speedup is nearly a factor of 25, with a reduction in disk space requirements by a factor of 30. Even for the CD-8 approximation, which is virtually exact, the calculation requires less than 8% of the disk space and is nearly five times faster than the conventional one.

C. Diuraniumendofullerene

The new CASSCF implementation is intended for systems that are not immediately feasible with conventional implementations. One such system is diuraniumendofullerene, $U_2@C_{60}$, which has been reported to possess a septet ground state (see Refs. 62 and 63 and references therein). An efficient implementation of multiconfigurational wave function methods is imperative in order to study the electronic structure of $U_2@C_{60}$.

We here calculate the CASSCF(6,18) wave function of the lowest-lying septet state of $U_2@C_{60}$ using CD and DF technology. We employ in all cases the relativistic ANO-RCC basis set of Roos *et al.*[64] for the U atoms and three basis sets for the C atoms, namely, the MIDI,[65] ANO-RCC,[64] and cc-pVDZ (Ref. 60) basis sets.

Although the active space chosen in this example is relatively large, restricting the calculation to septet spin symmetry reduces the number of configuration state functions to less than 10 000. The cost of the CASSCF wave function optimization is therefore completely dominated by the size of the AO basis set. Actual timings are reported in Table IV along with the disk space used to store the CD or DF vectors.

TABLE IV. $U_2@C_{60}$. Timings of CASSCF(6,18) calculations of the lowest septet state in C_i symmetry (N is the total number of AO basis functions, and M is the number of DF auxiliary functions, or CD vectors).

			Wall time (h)		
N	Type	M	Vector generation	CASSCF iteration	Disk/Gbyte
740[a]	CD-4	2997	6.0	0.3	2.7
	aCD-4*	3796	1.2	0.4	3.9
	aCD-4	3269	1.1	0.4	3.4
1040[b]	CD-4	4373	50.2	0.6	8.8
	aCD-4*	6516	11.5	0.8	13.6
	aCD-4	5104	9.5	0.7	10.7
1040[c]	CD-4	4349	11.5	0.5	8.4
	aCD-4*	5676	3.5	0.7	11.8
	aCD-4	4264	3.0	0.6	8.9

[a]U[ANO-RCC.$9s8p6d4f1g$],C[MIDI.$3s2p$].
[b]U[ANO-RCC.$9s8p6d4f1g$],C[ANO-RCC.$3s2p1d$].
[c]U[ANO-RCC.$9s8p6d4f1g$],C[cc-pVDZ].

We observe that the time required to perform a CD of the ERI matrix is substantially larger than that required to generate DF vectors. This is mainly due to the presence of four-center ERIs in the CD, whereas the DF vector calculation requires only three-center ERIs. It must be stressed that the generation of the auxiliary basis sets by CD of the atomic ERI matrix has no influence on the computational cost of calculating DF vectors. From the calculations using the two largest AO basis sets, both containing 1040 basis functions, we note that the computational cost depends not only on the size but also on the nature of the AO basis set. The ANO-RCC basis functions are defined by contractions of a much larger number of primitive functions than in the cc-pVDZ case and the ERI evaluations are therefore significantly more expensive for the former, regardless of whether four-center integrals are needed or not. The disk space consumption, on the other hand, is less sensitive to the nature of the basis set.

IV. CONCLUSIONS

We have presented a CASSCF implementation based on CD and DF approximations to the ERIs. The complexity of the CASSCF wave function requires that the ERIs are reproduced with uniform accuracy. While this is trivially fulfilled in the CD case, standard DF auxiliary basis sets constructed by data fitting of specific energy contributions are of no use. Instead, we employ auxiliary basis sets obtained by CD of the atomic ERI matrix, allowing a degree of error control which is almost as good as for the full CD. As explicitly shown by sample calculations, substantial computational savings are obtained compared to the conventional CASSCF implementation with no loss of accuracy.

ACKNOWLEDGMENTS

APPENDIX: REDUCED COST FORMULATION OF THE DF-CASSCF METHOD

Here we demonstrate that it is possible to compute the CASSCF inactive and active Fock matrices in terms of CD or DF vectors with a formal computational cost lower than the one discussed in Sec. II B. In Eq. (9) we have restricted the first index to be inactive while the second index is general. In this case we may as well compute the corresponding MO half-transformed Fock matrix:

$$F_{i\alpha} = 2({}^I F_{\alpha i} + {}^A F_{\alpha i}), \tag{A1}$$

where the general index is now in AO basis. The half-transformed inactive and active Fock matrices would then read

$$
\begin{aligned}
{}^I F_{\alpha i} &= h_{\alpha i} + \sum_k \left[2(\alpha i | kk) - (\alpha k | ik) \right] \\
&= h_{\alpha i} + 2 \sum_J L^J_{\alpha i} \sum_k L^J_{kk} - \sum_{Jk} L^J_{\alpha k} L^J_{ik} \\
&= h_{\alpha i} + 2 \sum_J L^J_{\alpha i} U^J - \sum_{Jk} L^J_{\alpha k} L^J_{ik},
\end{aligned}
\tag{A2}
$$

$$
\begin{aligned}
{}^A F_{\alpha i} &= \sum_{vw} D_{vw} \left[(\alpha i | vw) - \frac{1}{2}(\alpha w | vi) \right] \\
&= \sum_J L^J_{\alpha i} \sum_{vw} D_{vw} L^J_{vw} - \frac{1}{2} \sum_{Jw} L^J_{\alpha w} \sum_v D_{vw} L^J_{vi} \\
&= \sum_J L^J_{\alpha i} V^J - \frac{1}{2} \sum_{Jw} L^J_{\alpha w} Y^J_{wi}.
\end{aligned}
\tag{A3}
$$

The half-transformation of the vectors in the primary space (inactive+active) scales as $(I+A)N^2M$ and is the most demanding in terms of operation count. Apart from that, the most expensive term to be computed is the exchange part of the inactive Fock matrix, scaling as I^2NM, which is much smaller then the cost for the exchange term in the AO basis (IN^2M), assuming $I \ll N$.

Finally, also for Eq. (13) we can compute the corresponding half-transformed matrix:

$$F_{v\alpha} = \sum_w D_{vw}{}^I F_{\alpha w} + Q_{v\alpha}. \qquad (A4)$$

The first term involves a block of the inactive Fock matrix $^I F_{\alpha w}$ which can be easily obtained by complementing $^I F_{\alpha i}$ in the active orbital space

$$^I F_{\alpha w} = h_{\alpha w} + 2 \sum_J L_{\alpha w}^J U^J - \sum_{Jk} L_{\alpha k}^J L_{wk}^J, \qquad (A5)$$

with a cost scaling as $IANM$ in the leading term (exchange).

Hence, by constructing the inactive and active Fock matrices from the half-transformed DF vectors as in Eq. (A3), the saving in operation count for the leading term is about 50% for large basis sets. As HF wave function optimization can be considered a special case of the CASSCF one, these conclusions apply to HF as well.

[1] B. O. Roos, in *Advances in Chemical Physics; Ab Initio Methods in Quantum Chemistry-II*, edited by K. P. Lawley (Wiley, Chichester, England, 1987), Chap. 69, pp. 399–445.

[2] L. Gagliardi and B. O. Roos, Nature (London) **433**, 848 (2005).

[3] K. Andersson, P.-Å. Malmqvist, B. O. Roos, A. J. Sadlej, and K. Wolinski, J. Phys. Chem. **94**, 5483 (1990).

[4] P.-Å. Malmqvist, R. Lindh, B. O. Roos, and S. Ross, Theor. Chim. Acta **73**, 155 (1988).

[5] B. O. Roos, P.-A. Malmqvist, and L. Gagliardi, J. Am. Chem. Soc. **128**, 17000 (2006).

[6] L. Serrano-Andrés and M. P. Fülscher, J. Am. Chem. Soc. **120**, 10912 (1998).

[7] F. Aquilante, K. P. Jensen, and B. O. Roos, Chem. Phys. Lett. **380**, 689 (2003).

[8] F. Aquilante, V. Barone, and B. O. Roos, J. Chem. Phys. **119**, 12323 (2003).

[9] L. De Vico, M. Garavelli, F. Bernardi, and M. Olivucci, J. Am. Chem. Soc. **127**, 2433 (2005).

[10] L. Serrano-Andrés, M. Merchán, and R. Lindh, J. Chem. Phys. **122**, 104106 (2005).

[11] L. Blancafort, D. Gonzalez, M. Olivucci, and M. A. Robb, J. Am. Chem. Soc. **124**, 6398 (2002).

[12] A. Migani, M. J. Bearpark, M. Olivucci, and M. A. Robb, J. Am. Chem. Soc. **129**, 3703 (2007).

[13] N. H. F. Beebe and J. Linderberg, Int. J. Quantum Chem. **7**, 683 (1977).

[14] H. Koch, A. Sánchez de Merás, and T. B. Pedersen, J. Chem. Phys. **118**, 9481 (2003).

[15] T. B. Pedersen, A. M. J. Sánchez de Merás, and H. Koch, J. Chem. Phys. **120**, 8887 (2004).

[16] F. Aquilante, T. B. Pedersen, and R. Lindh, J. Chem. Phys. **126**, 194106 (2007).

[17] I. Røeggen and E. Wisløff-Nielsen, Chem. Phys. Lett. **132**, 154 (1986).

[18] D. W. O'Neal and J. Simons, Int. J. Quantum Chem. **36**, 673 (1989).

[19] S. Wilson, Comput. Phys. Commun. **58**, 71 (1990).

[20] T. B. Pedersen, H. Koch, L. Boman, and A. M. J. Sánchez de Merás, Chem. Phys. Lett. **393**, 319 (2004).

[21] I. García Cuesta, T. B. Pedersen, H. Koch, and A. M. J. Sánchez de Merás, Chem. Phys. Lett. **390**, 170 (2004).

[22] I. García Cuesta, T. B. Pedersen, H. Koch, and A. Sánchez de Merás, ChemPhysChem **7**, 2503 (2006).

[23] I. Røeggen, J. Chem. Phys. **124**, 184502 (2006).

[24] I. Røeggen, J. Chem. Phys. **126**, 204303 (2007).

[25] A. Öhrn and F. Aquilante, Phys. Chem. Chem. Phys. **9**, 470 (2007).

[26] B. Fernández, T. B. Pedersen, A. Sánchez de Merás, and H. Koch, Chem. Phys. Lett. **441**, 332 (2007).

[27] F. Aquilante and T. B. Pedersen, Chem. Phys. Lett. **449**, 354 (2007).

[28] I. García Cuesta, J. Sánchez Marín, T. B. Pedersen, H. Koch, and A. Sánchez de Merás, Phys. Chem. Chem. Phys. **10**, 361 (2008).

[29] F. Aquilante, P. Å. Malmqvist, T. B. Pedersen, A. Ghosh, and B. O. Roos, J. Chem. Theory Comput. **4**, 694 (2008).

[30] K. Pierloot and S. Vancoillie, J. Chem. Phys. **128**, 34104 (2008).

[31] J. L. Whitten, J. Chem. Phys. **58**, 4496 (1973).

[32] M. Feyereisen, G. Fitzgerald, and A. Komornicki, Chem. Phys. Lett. **208**, 359 (1993).

[33] O. Vahtras, J. Almlöf, and M. Feyereisen, Chem. Phys. Lett. **213**, 514 (1993).

[34] A. P. Rendell and T. J. Lee, J. Chem. Phys. **101**, 400 (1994).

[35] K. Eichkorn, O. Treutler, H. Öm, M. Häser, and R. Ahlrichs, Chem. Phys. Lett. **240**, 283 (1995).

[36] C. Hättig and F. Weigend, J. Chem. Phys. **113**, 5154 (2000).

[37] F. R. Manby, P. J. Knowles, and A. W. Lloyd, J. Chem. Phys. **115**, 9144 (2001).

[38] H. J. Werner, F. R. Manby, and P. J. Knowles, J. Chem. Phys. **118**, 8149 (2003).

[39] M. Sierka, A. Hogekamp, and R. Ahlrichs, J. Chem. Phys. **118**, 9136 (2003).

[40] A. Sodt, J. E. Subotnik, and M. Head-Gordon, J. Chem. Phys. **125**, 194109 (2006).

[41] F. Weigend and M. Häser, Theor. Chim. Acta **97**, 331 (1997).

[42] P. Deglmann, F. Furche, and R. Ahlrichs, Chem. Phys. Lett. **362**, 511 (2002).

[43] P. Deglmann, K. May, F. Furche, and R. Ahlrichs, Chem. Phys. Lett. **384**, 103 (2004).

[44] D. Rappoport and F. Furche, J. Chem. Phys. **122**, 64105 (2005).

[45] K. Eichkorn, F. Weigend, O. Treutler, and R. Ahlrichs, Theor. Chim. Acta **97**, 119 (1997).

[46] F. Weigend, A. Köhn, and C. Hättig, J. Chem. Phys. **116**, 3175 (2002).

[47] S. Ten-no and S. Iwata, Chem. Phys. Lett. **240**, 578 (1995).

[48] S. Ten-no and S. Iwata, J. Chem. Phys. **105**, 3604 (1996).

[49] F. Aquilante, R. Lindh, and T. B. Pedersen, J. Chem. Phys. **127**, 114107 (2007).

[50] D. E. Bernholdt and R. J. Harrison, J. Chem. Phys. **109**, 1593 (1998).

[51] F. Weigend, Phys. Chem. Chem. Phys. **4**, 4285 (2002).

[52] B. O. Roos, Int. J. Quantum Chem. **S14**, 175 (1980).

[53] F. Aquilante, T. B. Pedersen, H. Koch, and A. Sánchez de Merás, J. Chem. Phys. **125**, 174101 (2006).

[54] R. Polly, H. J. Werner, F. R. Manby, and P. J. Knowles, Mol. Phys. **102**, 2311 (2004).

[55] J. M. O. Matos, B. O. Roos, and P.-Å. Malmqvist, J. Chem. Phys. **86**, 1458 (1987).

[56] B. O. Roos, K. Andersson, and M. P. Fülscher, Chem. Phys. Lett. **192**, 5 (1992).

[57] J. Lorentzon, P.-Å. Malmqvist, M. P. Fülscher, and B. O. Roos, Theor. Chim. Acta **91**, 91 (1995).

[58] MOLCAS 7, University of Lund, Sweden, 2007 (see http://www.teokem.lu.se/molcas/).

[59] G. Karlström, R. Lindh, P. Malmqvist, B. O. Roos, U. Ryde, V. Veryazov, P. Widmark, M. Cossi, B. Schimmelpfennig, P. Neogrady, and L. Seijo, Comput. Mater. Sci. **28**, 222 (2003).

[60] T. H. Dunning, J. Chem. Phys. **90**, 1007 (1989).

[61] I. de P. R. Moreira and F. Illas, Phys. Chem. Chem. Phys. **8**, 1645 (2006).

[62] X. Wu and X. Lu, J. Am. Chem. Soc. **129**, 2171 (2007).

[63] I. Infante, L. Gagliardi, and G. Scuseria, J. Am. Chem. Soc. (unpublished).

[64] B. O. Roos, R. Lindh, P.-Å. Malmqvist, V. Veryazov, and P.-O. Widmark, Chem. Phys. Lett. **409**, 295 (2005).

[65] R. E. Easton, D. J. Giesen, A. Welch, C. J. Cramer, and D. G. Truhlar, Theor. Chim. Acta **93**, 281 (1996).